Overview of the NASA LISA Laser System Development

Anthony W. Yu[1], Molly E. Fahey[1], Kenji Numata[1], Yvonne Kandem Manewa[1], Ali Feizi[2], Frankie Micalizzi[1], Hua Jiao[1], Joseph Hart[1], Xiaozhen Xu[3], Stewart Wu[1], Kylan Jersey[4], Will Drobnick[5], Pat Burns[6], Jennifer Lee[7] and Scott Merritt[8]

[1] NASA Goddard Space Flight Center, Greenbelt, MD, USA
[2] AK Aerospace Technology Corporation
[3] Science Systems and Applications Inc. (SSAI)
[4] NASA Postdoctoral Program
[5] Avo Photonics, Horsham, PA, USA
[6] Fibertek Inc., Herndon, VA, USA
[7] BAE Systems Inc., Space & Missions Systems, Boulder, CO, USA
[8] Merritt Analytics, Manassas, VA, USA

E-mail: anthony.w.yu@nasa.gov

Received xxxxxx
Accepted for publication xxxxxx
Published xxxxxx

Abstract

NASA Goddard Space Flight Center (GSFC) is developing a Laser System (LS) for the Laser Interferometer Space Antenna (LISA) mission, led by the European Space Agency (ESA) with a launch date of 2035. The LS under development at NASA GSFC consists of a Laser Head (LH), a Frequency Reference System (FRS), and Power Monitor (PMON) detector assemblies. The LS development, which began in late 2016, follows the established NASA process in demonstrating the performance requirements through the develoment of various models to advance the Technology Readiness Level (TRL) [1]. The effort began with a successful demonstration of a laboratory breadboard (TRL 4) and has achieved a status of TRL-6 (flight-qualified) through rigorous testing and performance verification for space applications.

In this paper, we provide an overview of the development and roadmap for advancing the LISA LS toward spaceflight by the NASA GSFC. Optomechanical and electronic details of each component and subsystems are presented in this paper, as well as test results and technical challenges that have been or are being overcome. As the project progresses, more detailed results will be reported in future publications including representative scientific data in support of the LISA launch, which is planned for 2035.

Keywords: LISA, gravitational waves, spaceborne laser, fiber amplifier

1. Introduction

The LISA mission is led by ESA as a large-class mission in the Cosmic Visions Program.[2] LISA was adopted by ESA in January 2024. The spacecraft is being built and assembled by the industrial core team led by OHB together with Thales Alenia Space [3]. The LISA observatory consists of three spacecrafts (SCs) trailing the Earth in a heliocentric orbit. The SCs are configured in a triangular formation, with each side of the triangle spanning a distance of ~2.5 million km. The laser

 © xxxx IOP Publishing Ltd

sources enable the formation of optical interferometry between SCs. LISA uses a heterodyne laser interferometer to detect picometer-level length variation over the arm caused by the gravitational waves. Each SC contains two reference test masses, to which the spacecraft is controlled by the drag-free control system.

Key elements of LISA's instrumentation are provided by a collection of ESA member states and NASA [2, 4]. The scientific community is organized through an international consortium of scientists that brings together global expertise in gravitational wave astronomy. The LS is one of the three key elements of the LISA instrumentation provided by NASA, the others are the telescope [5] and the charge management device (CMD) [6]. The LS will provide a stable light source that enables the interferometric measurements used to sense the presence of passing gravitational waves. Telescopes on each of the SCs will allow the laser light to be efficiently transmitted and received across the 2.5-million-km distances between SCs [7]. The CMD will reduce the buildup of electric charge on the freely-flying LISA test masses, preventing unwanted electrostatic disturbances [6]. In addition to its hardware deliverables, NASA is developing the Ground Science Segments for ground operations in support of processing the telemetry and science products from the LISA constellation to identify and characterize individual gravitational wave signals. This data will be publicly available to the global scientific community to enable a wide array of scientific investigations.

In the current architecture, each SC contains one laser system (LS), which is composed of four laser heads (LH) and one frequency reference system (FRS). Two of the four LHs on each SC are nominal and active (LH1N & LH2N) and the other two LHs are redundant units (LH1R & LH2R) as shown in Figure 1. The FRS-O is a highly stable optical cavity that serves as a laser frequency (thereby length) reference.
There are three FRSs in the constellation. Only one of them is used as a frequency reference at a given time. One of the six active LHs will be designated as the constellation reference and frequency locked to the FRS on the same SC. The other five LHs are offset phase-locked to this reference laser as transponder lasers, acting as an amplifying mirror at the far SC. The other two FRSs are cold spares making the subsystem doubly redundant at the constellation level.

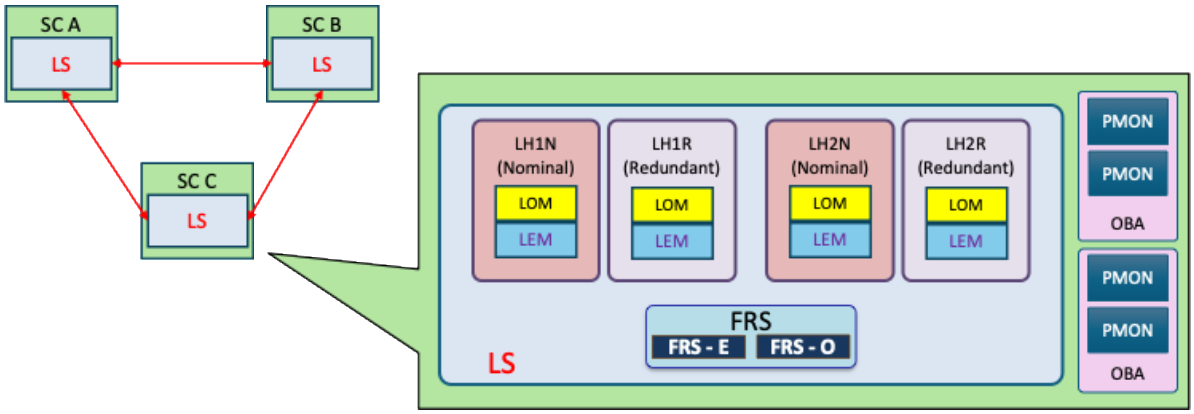

Figure 1. LISA Observatory consists of three spacecrafts (SCs), each SC carrying one laser system (LS) consisting of four laser heads (LHs) and one frequency reference system (FRS) as well as four power monitor (PMON) detector assemblies that reside on the optical bench assemblies (OBA).

Table 1. Summary of the LISA LS noise types (taken from the latest project documents) and mitigation strategies to meet project requirements. MO is the main oscillator, and the PMS is the phase measurement system.

Types of Noise	Requirements	Origin	Mitigation
Frequency noise	$S_\nu(f) \leq 30 \frac{Hz}{\sqrt{Hz}} \sqrt{1+\left(\frac{2\ mHz}{f}\right)^4}$ @ 0.1mHz~1Hz	Reference cavity length fluctuation due to temperature, laser cavity length fluctuation, quantum noise, etc.	Stable laser resonator (monolithic MO) and FRS-O, LH & FRS control loop provides frequency stabilization, LH & PMS control loop provides phase locking (stabilization).
Relative intensity noise (RIN)	$S_{RIN}(f) \leq 10^{-4} \frac{1}{\sqrt{Hz}} \times \sqrt{1+\frac{0.5\ mHz}{f}}$ @ 0.1mHz~100Hz	Excess current noise for the pump source, thermal fluctuations in the gain medium, quantum noise, etc.	PMON and LEM control loop provides RIN stabilization.
RF sideband phase noise	$S_\phi(f) < 60 \left(1+\frac{70\ mHz}{f}\right) \frac{\mu rad}{\sqrt{Hz}}$ @ 0.1mHz~1Hz	Optical length changes in the phase modulation waveguide, amplifier, and delivery fiber due to changes in ambient temperature, external noise coupled to system, etc.	Maintain thermal stability on LH, gain fiber and any external effects that could contribute to stress/thermal induced phase changes in modulation sideband.

Table 1 summarizes the types of noise present in the LS

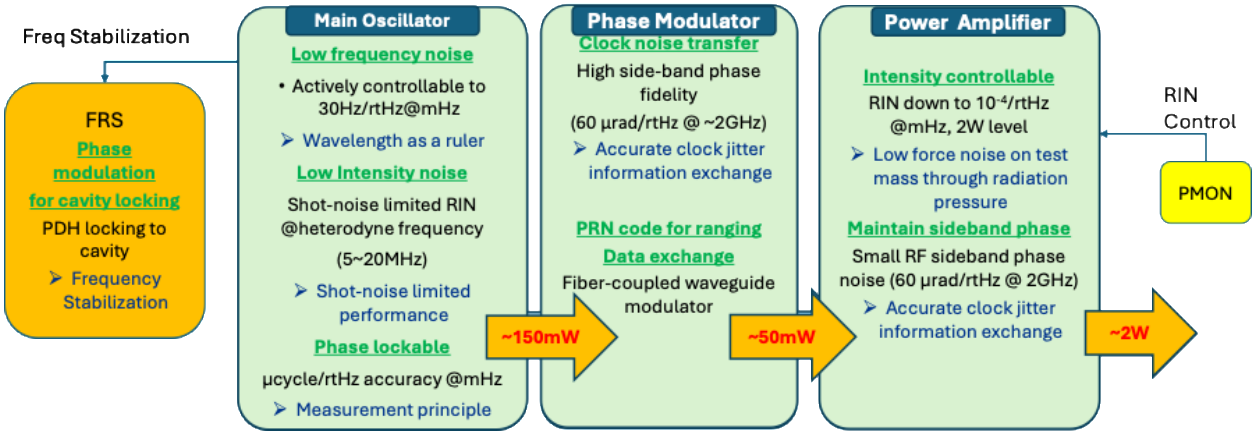

Figure 2. LH architecture and design philosophy.

Each LH consists of a laser optical module (LOM) and a laser electronics module (LEM). The power monitor (PMON) detector assemblies, located on the Optical Bench Assembly (OBA), are part of the LS. The OBA will be provided by the UK Astronomy Technology Centre (UKATC) for LISA [8]. The PMON picks up a small amount of laser light delivered by the LH to the OBA and fed back into the LEM for relative intensity noise (RIN) control of the laser power.

The LS development effort at NASA officially began in late-2016. Since then, the Lasers and Electro-Optics Branch at NASA GSFC has been developing and refining the design of the LISA LS. Currently the technology readiness level (TRL) of the NASA LISA LS is transitioning from 4 (lab testing) to 6 (prototype demonstration in a relevant environment) [1, 9]. In our context, a hardware item is described as TRL 4–6 when it is designed to meet the corresponding readiness-level requirements, using the designation primarily to indicate its intended maturity and development stage.

In 2021, NASA delivered a TRL-4 LOM to the Swiss Center for Electronics and Microtechnology (CSEM), under an ESA contract, for independent assessment of the NASA LH performance. Following a successful completion of the TRL-4 LOM evaluation campaign in late 2024, [10] NASA delivered a TRL-6 LOM and a TRL-5 LEM to CSEM in June 2025 for performance evaluation under vacuum conditions.

Our current technology development effort is focused on advancing the TRL of the LH, FRS, and PMON to TRL 6, a pre-requisit to flight implementation. The design of each of the subsystems within the LS meets the general requirements, such as size, weight, and power consumption (SWaP), operating and non-operating temperature ranges, vibration, shock, and radiation. The required LH output power of 2 Watt, throughout the mission lifetime, is delivered through a single-mode polarization-maintaining fiber to the OBA.

and our LH design strategies (Figure 2) to mitigate and minimize these noise sources for the LS to meet LISA requirements. The LISA LH working with FRS and PMON is designed to meet the low frequency noise, low intensity noise, and low radio frequency (RF) sideband phase noise as not to add length measurement errors through interferometric sensing noise, force noise on the test mass, and clock synchronization noise, respectively.

Another unique requirement is the long lifetime. Including testing and integration phase on the ground, cruise phase, nominal science operation phase, and extended science operation phase, 10~16 years of lifetime is required for the LISA laser. Each of the LHs, including the pump laser diodes and other critical components must have high enough reliability or redundancy to meet the unique lifetime requirement.

2. Laser System

The design philosophy of the LS is shown in Figure 2 where each part of the LS plays a key role in meeting the mission key requirements. And the functional block diagram of the LS is shown in Figure 3.

The main oscillator (MO) is a low frequency and intensity noise oscillator that is frequency locked to the FRS. The MO will also be interfaced with the Phase Measurement System (PMS) through the LEM on the LISA instrument for optical phase locking. The phase modulator (PM) located inside the LH is required to transmit reference clock information between spacecraft using a phase-modulation sideband at ~2.4 GHz. Without the clock noise exchange, the tiny gravitational wave signal would be buried in the clock noise on the three SCs. Such GHz-level phase-modulation can be added only by a waveguide-based electro-optic modulator, which has an input power limitation of ~400 mW at best with current technology. The fiber-based main oscillator power amplifier

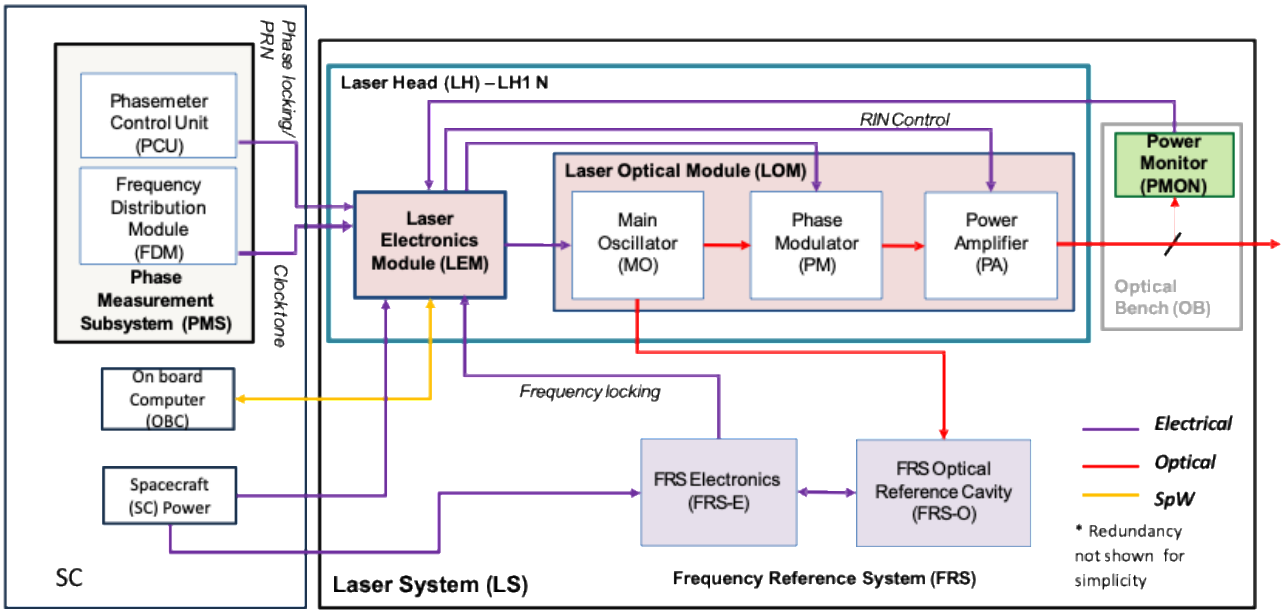

Figure 3. Functional block diagram of the LS and interfaces with other subsystems on the LISA observatory.

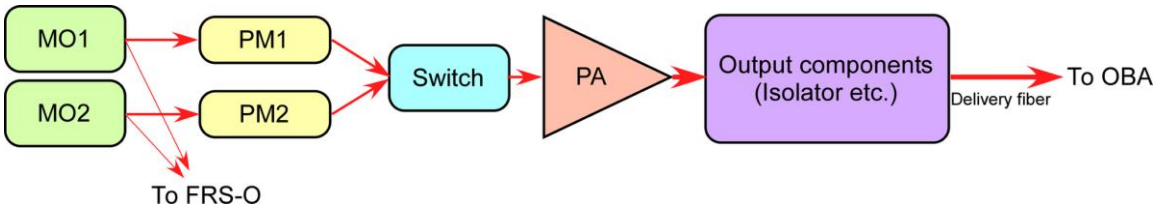

Figure 4. LISA LOM optical layout.

(MOPA) laser transmitter naturally overcomes this limitation. The power amplifier (PA) module provides the 2 W needed by the mission. The RIN from the PA is read out by the PMON located on the OBA. The PMON output is interfaced with the LEM on the LH to suppress the PA RIN.

3. Laser Head

3.1 Laser Optical Module (LOM)

The LOM consists of all the optical components and subsystems of the LH. The LOM enclosure is designed to be pressurized through the life of the mission. To meet the mission lifetime requirement, there are two MOs and two PMs for redundancy as shown in Figure 4. Only one MO/PM will be used at any one time and is selected by a low power optical switch. The "seed" light is amplified by a forward-pumped fiber power amplifier. The amplified light goes through the high-power isolator and the high-power tap coupler and provides the 2-W optical power for the mission.

To prevent the amplifier from catastrophic damages, especially unexpected lasing, multiple protection mechanisms have been implemented in the LH architecture. They included (1) the "scram" laser located inside the PA module, which quickly turns on to extract any excess optical gain from the gain fiber in the event that the seed power is lost, and (2) the fast PA pump shutdown mechanisms when the loss of seed or backward lasing is detected by the monitor photodiodes. To extend the lifetime, each MO has two 808-nm pump single-mode diodes that are hot redundant. They both operate at ~1/3 of their maximum operating current for derating. The PA uses three 976-nm multimode fiber-coupled pump diodes, where one will be used in nominal operation and the other two are cold redundant. Under nominal operation, the 976 nm pump is highly derated and operates at ~1/4 of its maximum operating current. Each PA pump laser diode has three internal emitters. Since the MO has enough output power to seed the single-stage PA, this design does not involve a "pre-amplifier" stage.

This single-stage design reduces numbers of electro-optical components and the overall system complexity. The typical input power to the amplifier is ~80 mW in the current single-stage design. The MO needs to emit ~200 mW of optical power in this case due to the insertion loss of the optical chain. The phase modulator must withstand such high input power

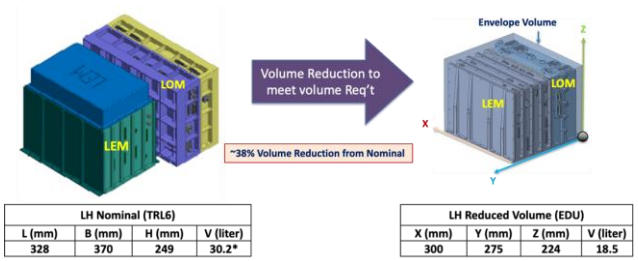

Figure 5. (left) TRL-6 LH and (right) the EDU LH designs. The linear dimensions and volumes shown are the as-designed parameters for the TRL-6 and EDU LHs to meet the requirements shown in Table 2.

level over long term (~10 years) operation with minimal degradation.

Figure 5(left) shows a TRL-6 LH mechanical design meeting the volume allocation as specified in the ESA TRL-6 Laser Demonstrator Requirements Document [11]. However, the ESA's volume allocation for the LISA flight laser requirements [12] has substantial differences and continued to evolve to the current set of requirements captured in the ESA Payload Requirements Document (PRD) and the Interface Requirements Documents (IRDs) [13, 14].

NASA undertook a parallel design phase during the TRL-6 LH development to reduce the volume of the LH to meet the LISA flight laser requirements as catpured in [12, 13, 14].

Table 2. Summary of LH models developed at NASA based on ESA's not-to-exceed (NTE) linear dimensions and volumes requirements in the PRD and IRD for the LH designs.

Model	Linear Dimensions			Volume	Req't References
	X (mm)	Y (mm)	Z (mm)	V (Liter)	
TRL-6	350	350	300	36.8	11
EDU	350	255	270	24.1	12, 13, 14

Table 2 summarizes the various models and corresponding not-to-exceed (NTE) dimensions and volumes developed at NASA meeting different evolving requirements since the start of our effort. The new LH design, designated as the Engineering Design Unit (EDU), is shown on Figure 5(right) and is being planned for fabrication and complete assembly by the end of 2025. For both the TRL-6 and the EDU LH designs, we adopted a "clamshell" design for the LOM where two slices are built separately and put together at the end of the build. The MO slice and the PA slice can be built separately, allowing for a streamlined build process. The LOM enclosure is pressurized with >1 atm of clean dry air and sealed with an O-ring and hermetic electrical connectors and optical fiber feedthroughs.This design takes into account that most of the commercially available laser fiber optic components are not hermetically sealed for vacuum operation. The internal pressure of the LOM will be monitored continuously during

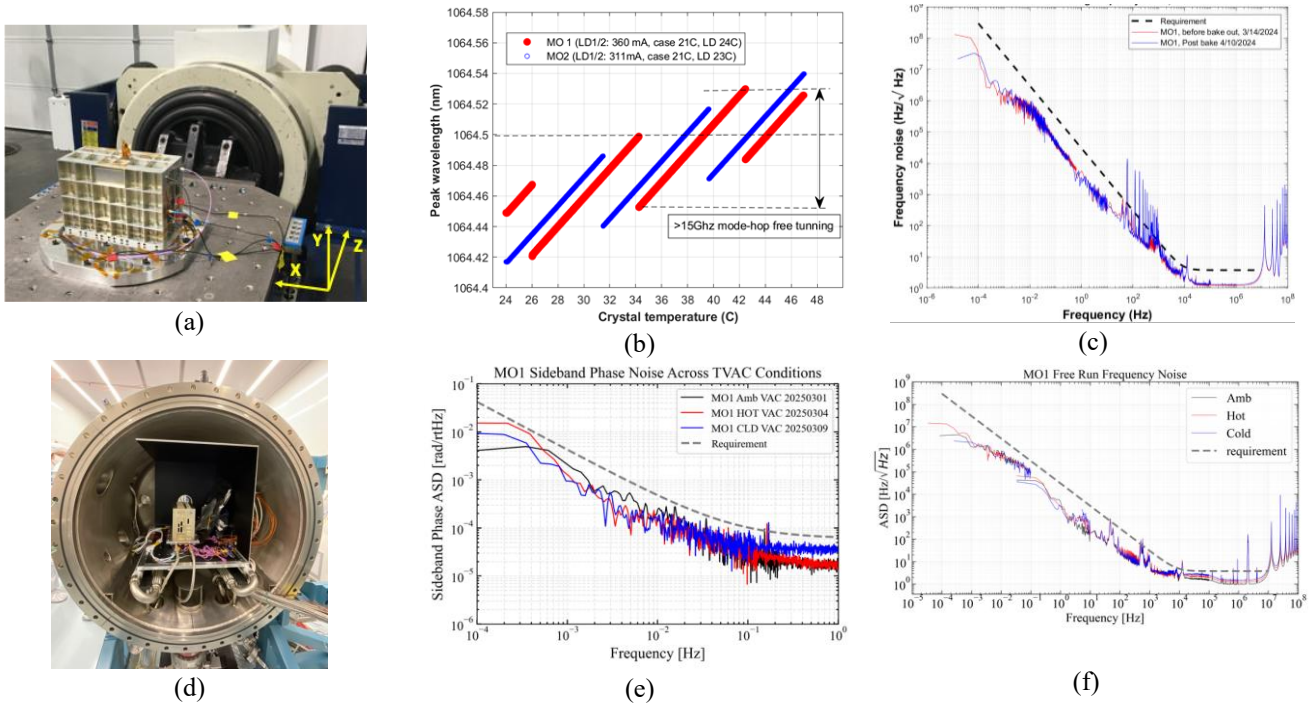

Figure 6. (a) Vibration test of TRL-6 LOM, (b) MO frequency tuning as function of crystal temperature, (c) free running frequency noise of the TRL-6 LOM, (d) TRL6 LOM inside the TVAC chamber; Post TVAC test results of TRL-6 LOM: (e) MO1 sideband phase noise over three different plateaus in TVAC and (f) free running frequency noise of the TRL-6 LOM.

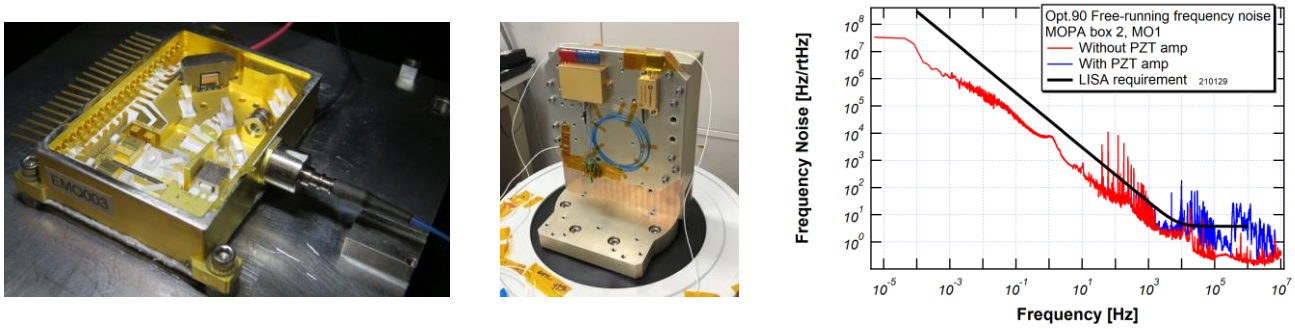

(a) (b) (c)

Figure 7. (a) The µNPRO MO as packaged. (b) Completed µNPRO MO package under vibration test. (c) Frequency noise of the µNPRO MO meeting the frequency noise requirements. The spikes at frequencies > 10 Hz are due to electrical line noise from the laser drivers and the measurement system. The excess noise above 10kHz on the blue trace is from the high voltage amplifier, which is not used in the LEM.

(a) (b) (c)

Figure 8. (a) TRL-6 PA package on a ground support equipment (GSE) chiller plate and (b) detector board as built for the TRL-6 LH. (c) The improved PA module design for the EDU LH combines both the PA and detector board in a single unit.

the environmental tests and long-term life aging tests. These procedures have been adopted in other GSFC-built space lasers.

The TRL-6 LOM went through vibration and thermal vacuum cycling (TVAC) testing as part of the TRL-6 qualification process. Figure 6(a) shows the vibration test of the TRL-6 LOM. Figure 6(b) shows the MO frequency tuning performance and Figure 6(c) shows the frequency noise performance before and after the bakeout. Figure 6(d)-(f) show the TRL-6 LOM TVAC campaign and representative results. All performance metrics remained nominal.

3.1.1 Main Oscillator

As for the MO, we have identified that the monolithic non-planar ring oscillator (NPRO) [15] as the most promising architecture for its lowest noise and simplicity. Our custom designed NPRO, denoted as micro NPRO (µNPRO) to reduce SWaP, has been shown to satisfy the stringent LISA MO requirements. The µNPRO prototype breadboard is conceived and demonstrated at GSFC [16 , 17 , 18] and the optomechanical package is designed and built by Avo Photonics Inc. in partnership with GSFC [19, 20].

Figure 7(a) shows the TRL 6 MO package as built. Since our earlier TRL-4 work, the TRL-6 design has been significantly improved. The TRL-6 MO package is hermetically sealed with an internal getter, similar to commercial hermetically sealed butterfly laser packages. We used two types of flux-free solders wherever possible to minimize slow drift of components. The package is mechanically stiffened to avoid misalignment due to package distortion. The µNPRO crystal has been redesigned to have a lower threshold, stable beam size, higher fiber coupling efficiency, and higher piezoelectric transducer (PZT) frequency tuning efficiency (>10 MHz/V) [21].

Following the updated build procedure and material, multiple MO packages have been built and passed all space qualification tests such as radiation, shock, vibration, and temperature cycling (Figure 7(b)). The 808-nm pump laser diode has been life-tested at our vendor (Eagleyard Photonics GmbH/) at CoS (chip on submount) level, and at GSFC at the pump-subassembly level. Figure 7(c) shows the MO frequency noise performance. The MO is capable of emitting >300 mW output power in fiber with low frequency noise and drift. They are realized by the small µNPRO crystal design and the precise temperature controls.

3.1.2 Power Amplifier

The PA is a forward-pumped fiber amplifier with 10-µm double-clad Yb gain fiber. The TRL-6 PA module for the

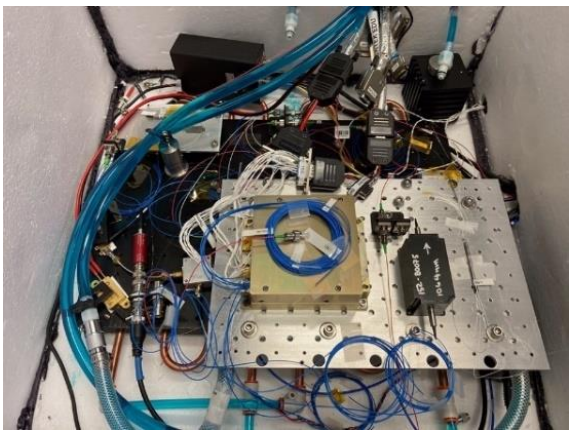

(a)

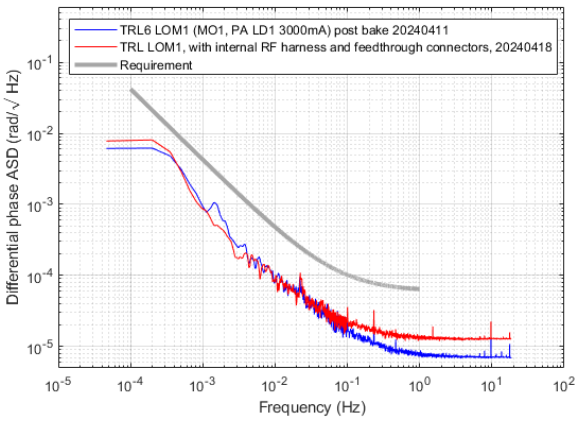

(b)

Figure 9. (a) RF sideband phase noise measurement setup at GSFC, (b) Measured RF sideband phase noise of TRL-6 LOM prior to vacuum bake out in advance of sealing the LH enclosure (red) and post bake out (blue).

TRL-6 LH is shown in Figure 8(a) that contains the gain fiber and pump diodes and is separated from the detector board (Figure 8(b)) that contains the scram laser and health monitoring photodiodes. Multiple optical monitoring channels were added in the EDU LH for better characterization and to prevent the amplifier from being damaged.

The TRL-6 PA module has been environmentally tested and characterized before and after thermal cycle and vibration test at 18.5g rms without any change in performance. Long-term testing of the amplifier is starting both at the component level and at the unit level. For the EDU LH, the PA module has been redesigned to a more compact unit and the separate detector board in the TRL-6 design has been integrated into a single module as shown in Figure 8(c).

The RF sideband phase noise added by the PA is a key parameter for the LISA laser. It directly affects LISA's science performance since the RF sideband phase noise limits the ability to synchronize reference clocks between the three SCs. We have started a dedicated experimental program at GSFC and a theoretical investigation at University of Illinois Urbana-Champaign (UIUC) to study the origin of the RF sideband phase noise. At UIUC, the study objectives are to investigate the linear and RF sideband phase noises. The linear phase noise manifests as the frequency noise in the laser wavelength. The RF sideband phase noise is the random variation in the relative phase between the carrier and its sidebands. The active and passive optical fibers serve as the gain medium of the LH and the delivery of signals throughout the transmitter to the OBA, respectively. These fibers are susceptible to both internal and external perturbations, which include, but are not limited to, changes in temperature from the system or surrounding environment, mechanical vibrations, and radiation-induced optical damage.

Throughout the whole LH, the passive fiber, inside and outside the LH, is one of the more susceptible components to these sources of noise because the fiber temperatures cannot be precisely controlled across the entire length. UIUC analyzed these effects due to both internal and external temperature fluctuations on the passive fibers currently being used in the LH. The UIUC results showed that the coupling of the external thermal environment into the passive fiber contributed to the RF sideband phase noise [22]. We are currently investigating the contribution to the phase noise from the optical fibers internal to the LOM. These results provide the guidelines and thermal stability requirements for the SC environment on the LISA Instrument.

Figure 9(a) shows the GSFC setup to measure the RF sideband phase noise of the PA and/or MOPA. The noise floor of the measurement system has been improved by temperature stabilizing all components, including RF electronics, and by thermally isolating everything from the room temperature fluctuation. Figure 9(b) shows the measurement results of TRL-6 LOM before and after the vacuum bake out of the assembly completed before the sealing of the LH enclosure. The result shows that, in a proper thermal environment, the RF sideband phase noise of the LH can meet the LISA requirement.

3.1.3 Other LOM Components

We selected MOPA components with previous space flight heritage whenever possible. They included fused fiber couplers, monitor photodiodes, and the pressure sensor. Some other components do not have enough qualification data and are subjected to appropriate qualification processes at GSFC for LISA and future space applications.

For example, the high-power isolator used in the TRL-6 LH met the magnetic cleanness requirement, but the destructive physical analysis (DPA) showed quality and cleanliness concerns with its internal structure from this particular vendor. For the EDU LH we have selected a new vendor to provide a new part with low residual magnetic field and a ruggedized package with smaller footprint. We have worked with the isolator vendor and achieved very low magnetic field leakage

by arranging magnets around the isolator to cancel the large magnetic field generated by the permanent magnets in the device design.

For the TRL-6 LOM and FRS, we plan to use a ~20 GHz phase modulator that has been tested at high optical input power (~200 mW in our case), high temperature, and qualified for space use. Long-term testing in vacuum has shown no evidence of performance degradation. The optical switch is unique to our design required to switch between the nominal and redundant MOs. Although several commercial optical switches have been evaluated for space use [23], none were found to directly satisfy our optical, mechanical, and environmental requirements. We are working with a vendor to develop a hermetic, robust, and high reliability optical switch for the EDU LH. The detailed component test results will be reported in a separate publication.

3.2 Laser Electronics Module (LEM)

The GSFC's Electrical Engineering Division continues to develop the LEM for the LH as well as for the FRS-E. Figure 10 shows the TRL-5 LEM undergoing testing in combination with a GSE LOM. The current TRL-5 LEM for the TRL-6 LOM contains five cards in a single chassis, as shown in Figure 10, containing the laser diode drive card (LDDC), the MO/PA controller card (MPCC), the power distribution card (PDC), command and telemetry controller card (CTC), and the phase modulator combiner (PMC) card.

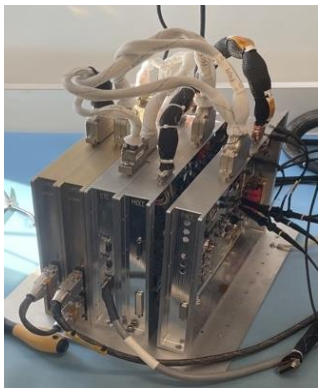

Figure 10. TRL-5 LEM undergoing testing.

The PDCs and CTC designs are based on previous space flight electronics. The PDCs convert the spacecraft's DC input to other required DC voltages for the other cards. In our design, the FPGA on the CTC will not require much computational power, since we do not have any complicated digital signal processing. A radiation-hardened FPGA with moderate size has been selected for this reason. We have developed TRL-4 and TRL-5 MO and PA controller cards based on laboratory prototype circuits, with special attention paid to minimizing circuit noise during the design. The TRL-6 versions are currently being designed and assembled with consideration of direct flight part replacements and parts availability.

Redundancy of each connection to the spacecraft, LOM, PMON, and other subsystems, is an important topic for the system reliability. We have agreed with ESA on the top-level and detailed connection architectures, considering failure and recovery scenarios. Initial testing of the TRL-5 LEM showed promise with performance meeting the LISA requirements. The decision was made not to proceed with an entirely new TRL-6 LEM design but rather to spend the resources to design a volume that fits within the EDU LH envelope, based on the TRL-5 LEM experience. The EDU LEM design is on track to complete production by end of 2025 for integration with the EDU LOM.

4. Frequency Reference System (FRS)

The FRS, which consists of a high finesse optical reference cavity (FRS-O) and electronics (FRS-E), will be used in concert with the LH to achieve the low frequency noise requirement.

4.1 Frequency Reference System-Optical Cavity (FRS-O)

The FRS-O is an improved version of the GRACE-Follow-On's (GFO) cavity built by BAE Systems Inc, formerly Ball Aerospace, which met the ranging noise requirement of 80 nm/√Hz [24 , 25], see Figure 11(a). The LISA cavity incorporates suggested changes from a risk reduction study funded by the NASA Physics of the Cosmos Study office (PCOS) and completed after the GFO deliveries. Additional improvements included an inner vessel containing the optical cavity is now vacuum compatible for ease of ground testing (cavity is vented to space on-orbit). The FRS-O interfaces with the LOM via an optical fiber where a small portion of the MO beam is delivered to the FRS-O for locking to the Fabry-Perot cavity with a cavity finesse of ~12,000.

4.2 Frequency Reference System-Electronics (FRS-E)

NASA GSFC is working with BAE in developing the FRS-E, see Figure 11(b). The FRS-E Frequency Control Card (FCC) interfaces with the FRS-O and the LEM and provides the electronics for locking and stabilization of the laser frequency. The Pound-Drever-Hall (PDH) locking scheme is implemented in FPGA for MO frequency tuning and allows for autonomous auto-locking and re-locking of the laser frequency.

The interface between the FRS, LH and spacecraft is shown in Figure 11(c). The FRS-E communicates with the LEM-CTC for command handling and sends analog control signals to the LEM-MPCC to control the MO's PZT (fast) and temperature (slow) tuning. The FRS-E contains GSFC-designed power supply card (LFPDC) that takes primary bus power and generates isolated secondaries.

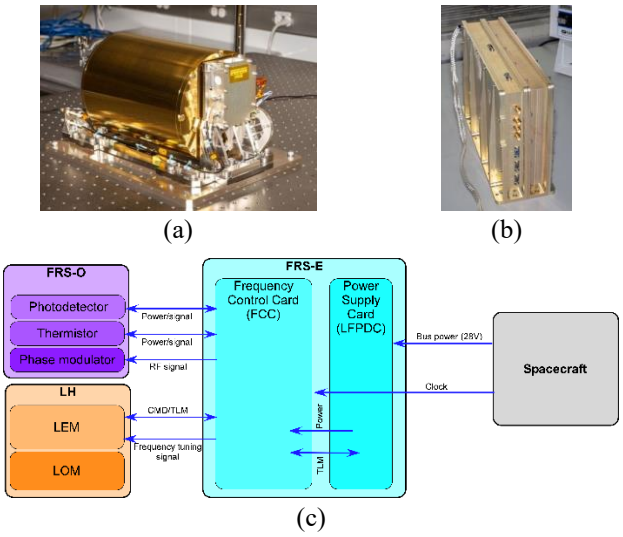

Figure 11. (a) Completed LISA TRL-6 FRS-O Cavity and (b) the TRL-5 FRS-E chassis that houses the GSFC provided LFPDC and FCC from BAE; (c) Block diagram of the interfaces between the FRS, LH, and spacecraft.

As of this writing, TRL-6 FRS-O has been successfully shown to meet the stringent LISA frequency noise requirements (Table 1) in a TVAC environment across all operating temperatures. It was driven by a TRL-5 FRS-E. The TRL-6 version of FRS-E will be installed in a TVAC chamber and tested with the TRL-6 FRS-O and MO by the end of 2025, and with EDU LH by spring 2026. Detailed results will be reported in subsequent publications.

5. Power Monitor (PMON)

The PMON is used to achieve the RIN requirement of ~100 ppm/√Hz at LISA's main observation frequency band. The PMON is located on the OBA, and it measures the optical power illuminating LISA's test mass precisely. The information is used to control the laser output power through a low-noise servo loop and the amplifier's pump current driver. While the PMON is located on the OBA, it is part of the LS deliverables by GSFC to the mission. There are two PMON assemblies per OBA. Each PMON assembly contains two detectors which serve as in-loop and out-of-loop detectors to control and monitor the optical power on the test mass, respectively.

A TRL-5 (EDU) PMON system was built as shown in Figure 12(a) and has been used to evaluate the photodiode and transimpedance amplifier in relevant thermal environment. For the TRL-6 (ETU) PMON development, the performance test setup was upgraded with the PMON on a Zerodur mock-up optical bench and multi-layer thermal shields in a dedicated vacuum chamber (Figure 12(b)) to minimize long-term power measurement errors. The setup is confirmed to have enough stability to achieve the 100 ppm/√Hz RIN requirement at LISA's observation frequency band (Table 1). The TRL-5 PMON was also tested together with the TRL-6 LOM set in a TVAC chamber and was shown to meet the RIN requirement as a LS. Detailed results will be reported in subsequent publications.

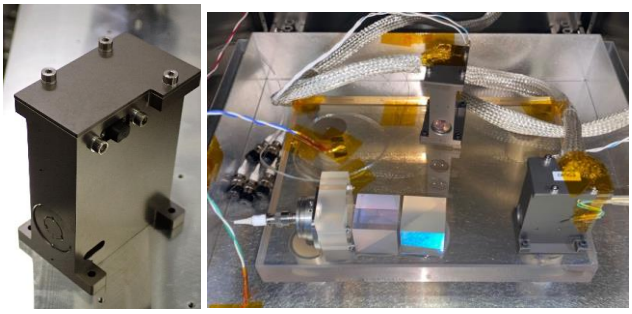

Figure 12. (a) TRL-5 PMON assembly and (b) Two TRL-5 PMONs integrated on a mock-up Zerodur optical bench. This bench is designed to go inside a dedicated vacuum chamber at GSFC for system level testing.

Multiple TRL-5 PMONs have been built by Avo Photonics Inc. and delivered to GSFC for evaluation. Avo Photonics has completed the TRL-6 (ETU) PMON design as well and will begin production in 2025. The ETU PMONs will be delivered to GSFC for evaluation and environmental qualification testing. Then two (2) ETU PMONs will be delivered to the UK OBA team for integration on the Engineering Model (EM) optical bench in early 2026.

6. Reliability

An effective reliability program requires more than life-testing components and subsystems; it also requires 1) establishing screening criteria, handling procedures, installation procedures, test procedures, and operating conditions or set points, and 2) understanding the physics of failure of relatively high-risk components so that the conditional probability of failure is minimized. It is not enough to design a reliability program that simply measures failure in time (FIT) rates, it must also guide the design of the screening protocols and provide proof (or disproof) of the efficacy of the screens, procedures and choice of operating conditions. [26]

We have devised a plan that calls for grouping components by *a priori* estimates of their FIT rates then establishing advanced test and screening methods. The *a priori* FIT rate estimates are obtained from multiple sources including literature surveys, vendor data, industry experience, and previous life-test measurements. The components are grouped into Groups 1, 2, and 3, as defined below.

6.1 Group Definitions and Methodology

Group 1

Definition: Those components which are either critical or for which one must both use very stringent or extraordinary test and screening techniques and analysis of the physics-of-failure to reduce the a posteriori FIT rate, ideally to less than 100.

Methodology: Components will be subjected to physics-of-failure analyses that address infant mortality, random failure, and wear-out mechanisms to support the selection of test, screening and burn-in criteria, lifetest design, and End-of-Life (EOL) calculations, respectively.

Group 2

Definition: Those components, for which normal screening techniques can reduce the conditional or *a posteriori* FIT rate (i.e., the FIT rates expected after passing the screen) to less than 100.

Methodology: Components and modules, e.g., the 2x1 switch, isolator-collimator, and NPRO TEC will be life tested and analyzed.

Group 3

Definition: Components, usually passive, with *a priori* FIT rates less than 100.

Methodology: The test plan for Group 3 components includes 100% functional testing. The plan also calls for Process Failure Modes and Effects Analysis (PFMEA) to ensure that our handling, testing, and installation processes do not introduce latent defects or damage.

Table 3 shows some of the LH components that we identified per our grouping definitions. Not all components used in the LH are shown. We have concentrated our program on Group 1 components since they are deemed most critical. Group 1 components are subjected to individually tailored aging campaigns to assess their reliability for use in the LISA LH design. A comprehensive paper is being prepared to describe the reliability approach we undertook for the LISA LH. It is a subject of future publication. Here, we will briefly describe our approach for two of our Group 1 components – the MO and PA pump diodes.

6.2 Implementation

The long-term aging tests of the pump laser diodes in the MO and PA have been carefully designed, given their critical role in ensuring long-term reliability. The sample size, test conditions (temperature and current), and corresponding acceleration factors were systematically determined during the experiment design phase.

Table 3. Examples of LH component Groups.

	Subassembly	Component or Element	Priority	Before Estimated FIT Rate, peak, 90%, 16 year	After Estimated FIT Rate, Advanced Screen
Grp 1	Main Oscillator	Pump Laser Diodes, 808 nm	10	2000	200
	Power Amplifier	Pump Laser Diodes, 976 nm	10	500	50
	Power Amplifier	Pump Combiner (TFB)	9.5	300	30
Grp 2	Integrated Module	Phase Modulator	10	80	15
	Main Oscillator	Optical Isolator	8	75	10
	Power Amplifier	Optical Isolator	8	75	10
	Main Oscillator	PZT Element	8.5	60	6
Grp 3	Power Amplifier	Cladding Power Stripper	8	50	5
	Main Oscillator	Nd:YAG	5	50	5
	Main Oscillator	Polarization Combiner	2	40	4
	Power Amplifier	Mode Filed Adapter	8	20	20

The MO pump diodes went through two sets of >5000-hour tests at high stress levels at Eagleyard Photonics as mentioned earlier. Each sample size was 20. The MO pump diodes were also tested at the pump sub-mount level at low-to-mid stress level. Based on the current results, we anticipate that there will be no failure due to the gradual degradation (1 dB power loss) during the mission if the diodes are de-rated as planned.

Table 4. Status summary of the LOM component testing (as of 2024). "X": completed. "P": planned. "-" : minimal contribution to magnetic cleanliness and will be tested as a whole once integrated at the LOM level.

Components	Construction Analysis	Accelerated life test	Gamma Radiation	Proton Radiation	Thermal Cycling	Vibration	Shock	Magnetic Field Test	Outgassing Test
MO - µNPRO	X	X	X		X	X	X	X	X
808nm pump diode	-	X	X	X		X		-	
Phase Modulator	X	X	X	X	P	X		-	X
Optical switch	X	P	X	X	X	P	X	-	X
Pump combiner (TFB)	X	P	X		X	X	X	-	X
976nm Pump Diode	X	X	X	X	P	P		-	X
Gain fiber	-	P	X					-	X
Optical Isolator (High Power)	X	X	X	X	X	P	X	P	X
Optical Isolator (Low Power)	X	P	X		X	X	X	P	X
Photodiode		P	X	X	P	X		-	X
Scram laser			X	X				-	X
Tap couplers		X	X		P	X	X	-	X
Pump filter			X		X	X	X	-	X
Circulator		P	X		X	X	X	-	X
Mode Field Adapter			X		X	X	X	-	X

A third reliability test at Eagleyard Photonics has been performed to evaluate sudden failures and the wafer dependency thereof. An > 8000 hour aging test investigating

wafer diversity on 40 pump laser diodes from three different wafers was performed. All samples behaved and endured as expected when stressed at acceleration factors ranging from 16 to 35. We are analyzing the test data and preparing a report that will be published at a later date.

The PA pump laser diodes were previously tested for another space mission but we are repeating the tests at operating conditions relevant for LISA. The same pump laser diode is also being tested by ESA at a high stress level under vacuum, and the reliability information has been actively exchanged. The baseline vendor for the PA diodes has relocated to a new factory and the production line is under qualification. Currently we are testing and qualifying diodes from two other vendors as replacements in case there is a delay on the production qualification from our baseline vendor. We intend to publish these results later, subsequent to the final selection of the PA pump laser diode in early 2026.

For all the components in other groups, we performed component-level analysis and testing, and theoretical analyses. They include functional testing, environmental testing (radiation, vibration, temperature cycle), magnetic field testing, destructive physical analysis (DPA), and life aging tests. Table 4 summarizes the status of the component-level testing and analysis. Our upcoming activities include LOM-, LEM-level life aging, additional component testing, especially under high power for the phase modulator and PA output optics, and long-term non-operating condition tests.

7. End-to-end testing of the NASA LS

Since the delivery of the TRL-4 LOM to ESA and CSEM for independent performance verification, we have taken steps to advance the TRL of the overall LS and have completed integrated subsystem testing and end-to-end LS system level testing. This includes 1) optical performance test of TRL-6 LOM and TRL-5 LEM under thermal cycling; 2) end-to-end test of the LH and the ground support equipment (GSE) FRS, driven by TRL-4 FRS-E provided by BAE. The GSE FRS is a laboratory cavity with similar FRS-O parameters and attributes; 3) end-to-end test of the LH with the GSE PMS

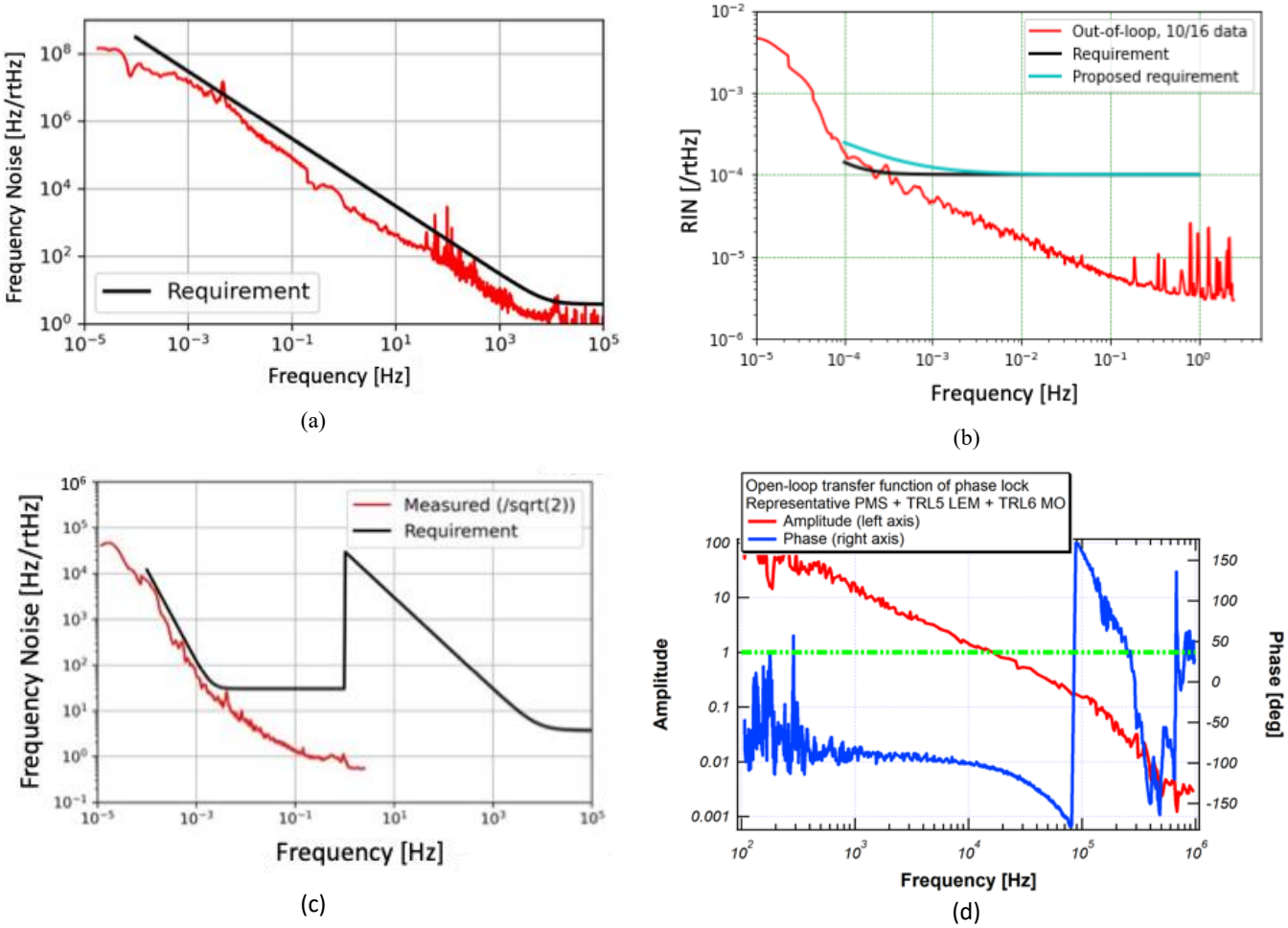

Figure 13. End-to-end testing of TRL-5 LEM and LH components: (a) TRL-5 LEM with TRL-6 MO free running frequency noise; (b) TRL-6 MO and TRL-4 PMON testing at low frequency band; (c) frequency noise performance of TRL-4 FRS and TRL-6 MO; and (d) open loop transfer function of TRL-6 MO, TRL-5 LEM and PMS.

provided by Albert Einstein Institute (AEI), and 4) optical performance test of the LH with the PMON subsystem built by Avo Photonics Inc. The FRS, PMS, and PMON provide necessary frequency stability, relative phase stability between lasers, and output power stability, respectively. Since they are all vital for the sensitive laser interferometry performed in LISA, it is necessary to perform system level testing by combining the LH and other subsystems, and to prove the optical performance at an early stage during the LS development.

Our recent work has successfully demonstrated the intra-connectivity of the LS, i.e. LOM-LEM, FRS and PMON, as well as critical external interface with the PMS to meet the LISA project performance requirements.

7.1 Free-running frequency noise performance

Figure 13 (a) shows the test result of the TRL-6 MO and TRL-5 LEM for free running frequency noise behavior. The TRL-5 LEM employs a low noise laser driver design based on space-compatible components with an ultra-low noise laser current driver selected from different architectures. The analog temperature controller on TRL-5 LEM is used to maintain heritage from TRL-4 LEM, however, a digital PID controller independently developed and tested will be implemented into the EDU LEM.

7.2 PMON and RIN stabilization loop performance

The TRL-4 PMON and TRL-6 MO were tested in vacuum to verify the PMON performance. The PMON was under passive temperature control and the RIN of the MO (after RIN stabilization) is shown in Figure 13(b). Low frequency RIN is challenging because it is difficult to maintain the RIN GSE stable over the test duration due to environmental temperature changes. The result shows the TRL-4 PMON meeting the 100ppm/√Hz LISA requirement.

7.3 FRS and frequency stabilization loop performance

The first FRS and LH testing is shown Figure 13(c) where the TRL-4 LOM (with TRL-6 MO inside the LOM) and TRL-4 FRS met the LISA's frequency noise requirement, ~30Hz/√Hz (Table 1). This proves the high stability and controllability of our custom MO design explained in 3.1.1.

7.4 Optical phase locking loop performance with PMS

We also performed interface test between the AEI PMS and the TRL-5 LEM and TRL-6 MO. The COTS FPGA loaded with the same phase meter algorithm was used in the test. The laser was successfully phase locked with residual phase noise meeting the in-loop performance with unity gain of 16.4 kHz and phase margin of 76° as shown in Figure 13(d). Therefore, the current LH design is compatible with the latest PMS logic to meet the phase lock performance requirements, which is critical to perform heterodyne interferometry.

Additional subsystem and end-to-end LS testing using higher TRL hardware have been completed at GSFC in the late 2024 – 2025 timeframe. The results of these tests will be reported in future publications.

8. Development Schedule

The TRL 6 demonstrator LOM completed thermal vacuum testing at GSFC in November 2024. The TRL-5 LEM and the TRL-6 LOM have been delivered to CSEM for another test campaign to begin in October 2025.

The EDU LH design is near completion and fabrication of this unit will be completed by the end of 2025 and proceed to go through environmental testing to advance the TRL of the EDU LH design to TRL6 in early 2026. The FRS development at BAE continues with the first TRL-6 FRS-O and TRL-5 FRS-E having been delivered to GSFC in October 2024. The second TRL-6 FRS-O and TRL-6 FRS-E are planned to be delivered to GSFC for further testing in late 2025. The ETU PMON design is continuing and planned to be completed and delivered to GSFC for testing in late 2025.

9. Summary

In this paper, we provided an overview of the LISA LS and the latest status of the LS system development effort.

Since 2016 we have continued the LISA laser development and have made key advancements to improve performance and reliability. We chose the MOPA architecture and have been developing technologies to meet these challenges. The LISA mission is unique and most challenging in terms of laser performance, which requires ultra-low noise laser systems and long lifetime.

The μNPRO MO is the most innovative component within the overall LH design [16-21]. It has been improved significantly and has passed all environmental tests with improved optical performance. The SWaP of the MO is designed so that two units can fit within the LH enclosure to provide redundancy necessary to meet the LISA mission lifetime requirements. The lessons learned from the TRL-4 LOM module have been fully incorporated into the TRL-6 and EDU LH designs. We are conducting performance tests, including RF sideband phase noise and relative intensity noise measurements, and environmental and life tests. We continue to perform and monitor life aging tests of components, subsystems, and the laser system. Multiple reliability analyses are ongoing to demonstrate lifetime of the laser using available test data.

As previously noted, all key LISA LS performance requirements have been satisfied from TRL 4 through TRL 6, and no fundamental limitations have been identified. Although long-term operation in the space environment cannot be fully verified on the ground, our dedicated reliability

efforts have substantially increased confidence in system robustness. Vendor and product availability remain significant considerations over the extended mission lifecycle, and appropriate measures have been implemented to mitigate associated risks. By addressing both engineering and programmatic challenges, we remain committed to fulfilling our responsibility to deliver the LISA laser as the U.S. contribution to the planned LISA launch in 2035.

References

[1]. https://www.nasa.gov/directorates/somd/space-communications-navigation-program/technology-readiness-levels/.

[2].https://www.esa.int/Science_Exploration/Space_Science/LISA.

[3]. https://www.ohb.de/en/news/ohb-to-construct-a-pioneering-spacecraft-constellation-to-capture-gravitational-waves.

[4]. https://lisa.nasa.gov.

[5]. Ritva A. Keski-Kuha, Ryan T. Derosa, Kevin R. Boyce, Theodore J. Hadjimichael, Joseph M. Howard, Joseph M. Ivanov, Timothy A. Johnson, Joshua G. Lutter, Jonathan C. Papa, Shannon R. Sankar, Andrew Weaver, "LISA telescope development status and flight design," Proc. SPIE 13092, Space Telescopes and Instrumentation 2024: Optical, Infrared, and Millimeter Wave, 130922C (23 August 2024).

[6]. Samantha Parry Kenyon et al. "Advanced charge control dynamics simulation for the LISA gravitational reference sensor", Class. Quantum Grav. **42** 055013 (2025).

[7]. P. Amaro-Seoane et al., "Laser Interferometer Space Antenna," Classical and Quantum Gravity, vol. 34, no. 24, p. 1 (2017).

[8]. William Brzozowski, David Robertson, Ewan Fitzsimons, Henry Ward, Jennifer Keogh, Alasdair Taylor, Maria Milanova, Michael Perreur-Lloyd, Zeshan Ali, Andrew Earle, Daniel Clarkson, Robyn Sharman, Martyn Wells, Phil Parr-Burman, "The LISA optical bench: an overview and engineering challenges," Proc. SPIE 12180, Space Telescopes and Instrumentation 2022: Optical, Infrared, and Millimeter Wave, 121800O (27 August 2022).

[9]. National Aeronautics and Space Administration, NASA Systems Engineering Handbook, NASA SP-2016-6105 Rev 2, Washington, D.C., (2017).

[10]. Lauriane Karlen, Emmanuel Onillon, Stefan Kundermann, Steve Lecomte, Kenji Numata, Michael Rodriguez, Anthony Yu, Micheal Born, Brian Shortt, Linda Mondin, "LISA NASA engineering design unit (EDU) laser head metrology," Proc. SPIE 13699, International Conference on Space Optics — ICSO 2024, 136992S (28 July 2025).

Acknowledgements

The authors acknowledge the support from the NASA SMD Science Mission Directorate (SMD) and PCOS. We deeply appreciate the collaborative effort from various GSFC engineering and science directorates as well as continuing support from numerous vendors and contractors at GSFC. The authors would also like to thank ESA, AEI and CSEM for their continuing support of our LISA laser development.

[11]. ESA-LISA-EST-PL-RS-002, LISA laser system TRL6 demonstrator requirements, Issue/Revision 1.4, 27/07/2020.

[12]. ESA-LISA-EST-INST-RS-001, LISA Mission Laser System Requirements (TRL6 development), Issue/Revision 5.0, 31/03/2022.

[13]. ESA-LISA-EST-PL-RS-0001, LISA Payload Requirements Document (PRD), Issue 1.3, 22nd March 2024.

[14]. ESA-LISA-EST-LS-RS-0001, LISA Laser System to Platform Interface Requirements Document (IRD1), Issue 1.0, 26th March 2024; ESA-LISA-EST-LS-RS-0002, LISA Laser System and Interface Requirements Document (IRD2), Issue 1.0, 8th March 2024.

[15]. Kane, T. and Byer, R. L., "Monolithic, unidirectional single-mode Nd:YAG ring laser," Opt. Lett. 10, 65-67, 1985.

[16]. A.W. Yu, K. Numata, S. Merritt, B. Nelsen, D. Demmer, J. Goettler, T. Haslett, and T. Kane, "Micro-non-planar ring oscillator master oscillator for the NASA LISA laser transmitter," Proc SPIE 12777 (2023) 1277747, DOI: 10.1117/12.2690676.

[17]. Anthony Yu and Kenji Numata, "Micro non-planar ring oscillator with optimized output power and minimized noise in small package," US Patent US11394168B1, 19 July, 2022.

[18]. Thomas Kane, Kenji Numata, John Nightingale, "Piezo-Tuned Nonplanar Ring Oscillator with GHz Range and 100 kHz Bandwidth," US 2023/0238764 A1, 27 July 2023.

[19]. Julia Majors, David R. Demmer, Ryan Ehid, Thomas L. Haslett, Kenji Numata, Anthony Yu, Thomas Kane, Scott Merritt, Oleg Konoplev, and Thomas Haslett, "Laser Interferometer Space Antenna: Master Oscillator Packaging," Presented at the SPIE Photonics West, San Francisco, CA, Paper 11261-16, February 2020.

[20]. Anthony Yu, Kenji Numata, Scott Merritt, Bryan Nelsen, David Demmer, Jonathan Goettler, Tom Haslett, Thomas Kane, "Micro-non-planar ring oscillator master oscillator for the NASA LISA laser transmitter," Proc. SPIE 12777, International Conference on Space Optics — ICSO 2022, 1277747 (12 July 2023); https://doi.org/10.1117/12.2690676.

[21]. T. J. Kane, K. Numata and A. Yu, "Strain Tuning a Nonplanar Ring Oscillator by 3.5 GHz: Theory and

Experiment," in IEEE Journal of Quantum Electronics, vol. 61, no. 2, pp. 1-9, April 2025, Art no. 1700109.

[22]. Jennifer Campbell, Xiaozhen Xu, Demetrios Poulios, Molly Fahey, Kenji Numata, Anthony Yu, Peter Dragic, "Investigation into the origin of the RF phase noise for the LISA laser transmitter," Proc. SPIE 12865, Fiber Lasers XXI: Technology and Systems, 1286508 (12 March 2024).

[23]. D. Poudereux, L. Aboussouan, F. Cazaux, A. Desportes, and A. Roda, "Evaluation of optical switches for Space applications," in Proceedings of SPIE — Smart Structures + Nondestructive Evaluation (SPIE 11180), Proc. SPIE 11180, 111807H, (2019).

[24]. K. Abich et al., "In-Orbit Performance of the GRACE Follow-on Laser Ranging Interferometer," Phys. Rev. Lett. 123, 031101 (2019).

[25]. R. Thompson et al., "A flight-like optical reference cavity for GRACE follow-on laser frequency stabilization," 2011 Joint Conference of the IEEE International Frequency Control and the European Frequency and Time Forum (FCS) Proceedings, San Francisco, CA, USA, 2011, pp. 1-3, doi: 10.1109/FCS.2011.5977873.

[26]. A. Yu, et al., "Progress and Plans for a US Laser System for the LISA Mission," Presented at 2nd International Workshop on Space-Based Lidar Remote Sensing Techniques and Emerging Technologies, Milos, Greece, 07 June 2018.